An experimental investigation on contact behaviour during structural pounding

S. Khatiwada, N. Chouw & T. Larkin

The University of Auckland, Auckland, New Zealand.

2014 NZSEE Conference

ABSTRACT: Current numerical force models of pounding assume that the supporting elements e.g. columns, shear walls etc. behave as flexure-only spring and do not include the effects of the axial and shear properties. They are based on impact experiments, where the energy loss is normally calculated from the coefficient of restitution measured from impact between spheres or bars suspended as pendulums. However, the high frequency excitation imposed by the pounding can activate shear and longitudinal modes of the colliding floors. This study presents the variation of impact-induced acceleration and coefficient of restitution when the support conditions are changed. Impact experiments are conducted between two steel beams for three support conditions i.e. when both the beams are suspended from overhead girder with cables; when one beam is suspended and the second beam is supported by columns; and when both the beams are supported by columns. Numerical simulations are carried out for all three cases with nonlinear viscoelastic and modified Hertzdamp models. It is shown that the change in support produced a substantial change in the pounding-induced acceleration and coefficient of restitution. However, the numerical simulations cannot reproduce such changes.

1 INTRODUCTION

Post seismic surveys have observed damage to structures as a result of collision between adjacent structures (Chouw and Hao 2012; Hamada *et al.* 1999; Rosenblueth and Meli 1986). Such collisions can be between two adjacent structures (Anagnostopoulos 1988; Kasai and Maison 1997) or between adjacent parts of a structure (Chouw and Hao 2008; Malhotra 1998). Seismic assessments of several cities have identified pounding as a significant vulnerability (e.g. Bothara *et al.* 2008; Jeng and Tzeng 2000) and structural pounding has been recognized as an urban seismic hazard.

Pounding occurs if the closing relative movement between adjacent structures or structural elements is less than the at-rest separation gap. The relative movement is due to the different natural periods of the structures (e.g. Chau and Wei 2001) or spatial variation of ground motion (e.g. Athanassiadou *et al.* 1994; Hao and Zhang 1999; Li *et al.* 2012). Even when the structures were designed with code specified requirements when they were built, they can be found susceptible to pounding as a result of implementing advances in knowledge. For instance, adjacent buildings which do not undergo pounding when simulated without foundation compliance effects, can collide together when these effects are included (e.g. Chouw 2002).

Numerical simulations of pounding mostly adopt a lumped-mass idealization where the floor masses are assumed to be concentrated at a point (Fig. 1). The collective storey stiffness is the sum of the flexural stiffness of the columns. An elastic or viscoelastic link and a gap element are introduced in between the floor masses. The gap is monitored throughout the simulation. When it becomes negative, the structures are in contact. When the structures are not in contact, they can be analysed normally as two separate buildings. A number of methods have been proposed to continue the simulation when they are in contact. Several studies (e.g. Athanassiadou *et al.* 1994) adopt the methods in stereomechanics, where the post-impact velocities of the floors are calculated from their masses and pre-impact velocities. Others (e.g Anagnostopoulos 1988) have applied the impact element method where the floors exert an equal and opposite force on each other until they separate. Many numerical expressions proposed to calculate this force. A detailed explanation of these methods can be found in references (e.g. Khatiwada *et al.* 2014). Several other procedures have been proposed e.g. Lagrange multiplier method (e.g. Papadrakakis *et al.* 1991) and combined time and Laplace domain analysis (Chouw and Schmid 1995). The dissipation of kinetic energy during impact is represented by the coefficient of restitution which is defined as the ratio of post-impact relative velocities of the floors to that before impact.

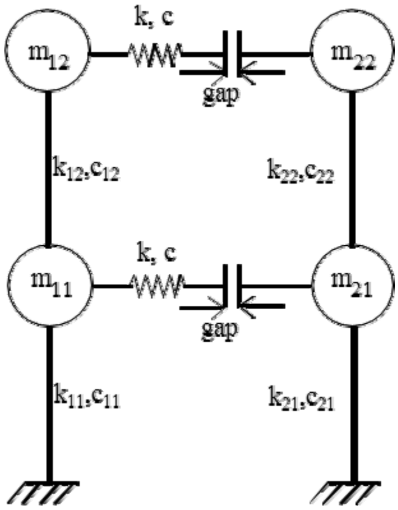

Figure 1. Lumped-mass model of pounding

Many experimental studies attempted to verify some numerical procedures. Papadrakakis and Mouzakis (1995) compared the predictions using the Lagrange multiplier method to that obtained from the experimental simulations. Filiatrault *et al.* (1995) attempted to verify the predictions from two finite element analysis software against experimental results, while Chau *et al.* (2003) adopted the nonlinear elastic force model from Hertz contact law. Jankowski (2010) compared the experimental displacement response with predictions from nonlinear viscoelastic model. In all cases, a substantial difference was observed between the numerical and experimental responses. Khatiwada *et al.* (2013a) compared the predictions of five different pounding force models against the displacement responses from shake table simulations. For each case all numerical models produced a similar response, which might be very close to the experimental results or might be substantially different. Chouw and Khatiwada (2013) presented the current limitations of seismic pounding studies in an attempt to explain these discrepancies between numerical and experimental results. One of the identified limitations is the exclusion of the effects of columns, walls or other structural members from the numerical force models.

The numerical force models consider the supporting structural members as lateral springs with stiffness equal to the sum of their flexural stiffness. This converts the idealized model in Figure 1 into the one in Figure 2. In addition, the models can be generalized as shown in Equation 1 which means that the columns do not have any effect on the calculation of pounding force. The equivalent damping ratio ξ and equivalent viscous damping c of the models are functions of k, $m_{i,j}$ and e, and their effect is included in Equation 1 by the independent variables.

$$F_j = f_1(m_{i,j}, k, \delta_j) + f_2(k, m_{i,j}, e, \delta_j, \dot{\delta}_j) \tag{1}$$

where F_j = the pounding force between the j^{th} stories; $m_{i,j}$ = the mass of the j^{th} floor of the i^{th} building; k is the stiffness of the contact interface; $\delta_j = u_{1,j} - u_{2,j}$ is the relative compression of the pounding stories; e is the coefficient of restitution; and $\dot{\delta}_j = \dot{u}_{1,j} - \dot{u}_{2,j}$ is the relative velocity of the pounding stories.

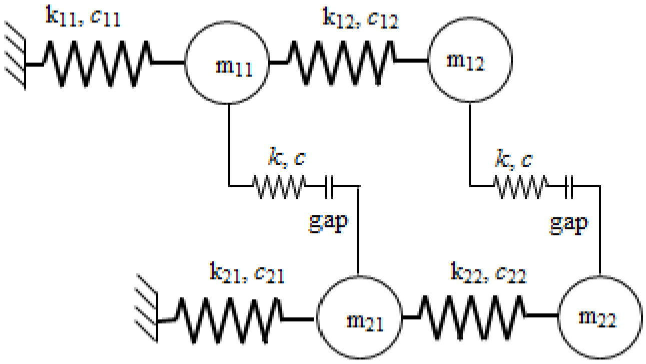

Figure 2. Lumped-mass model of pounding structures with idealized supports whose stiffness is obtained from the flexural properties of the columns.

The treatment of supporting structural members as lateral springs (Fig. 2) is equivalent to modelling them by the Euler-Bernoulli beam theory, instead of the Timoshenko beam theory which can include the effects of axial and shear properties of these structural members. This simplifies the computation; however, it ignores the effects of high frequency loads on these elements. Even the comparatively more detailed distributed-mass models of pounding (e.g. Cole *et al.* 2010; Malhotra 1998) do not incorporate the support structural members in force development. If their derived force models are used in computations, significant errors can occur. The calculated force time history may not be sufficient to cause a separation of the colliding masses. Thus, Malhotra (1998) recommended that the pre-impact velocities of the colliding diaphragms be adjusted to the predetermined post-impact velocities in incremental steps over the contact duration; and Cole *et al.* (2010) instead postulate an equivalent lumped-mass model which generates the same post-impact velocities as calculated from the distributed-mass model.

This absence of the effect of supporting structural members in the development of pounding force can cause significant errors because the pounding force causes compressive strains in the colliding diaphragms. The axial stiffness of the diaphragm will be higher if it is supported by a shear wall along its length than if it is supported by columns at the two ends. In addition, the response of brittle unreinforced masonry walls will be substantially different than that of RC or steel supports. Thus, numerical simulations cannot predict the widespread pounding damage to unreinforced masonry that was observed in 2011 Christchurch earthquake (e.g. Chouw and Hao 2012, Cole *et al.* 2012).

The study reported here presents recorded accelerations as a result of impact between two steel beams with various support conditions. The variation in the acceleration and coefficient of restitution are shown for three types of supports combinations i.e. impact between two pendulums, between pendulum and a frame, and between two frames. The acceleration response shows significant variation when the support conditions are altered.

2 EXPERIMENTAL SETUP

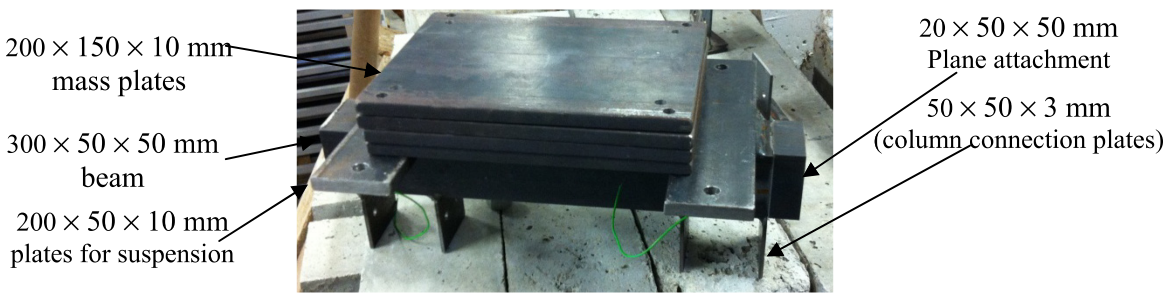

Figure 3. Steel beam constructed for the impact tests

Two 300 × 50 × 50 mm steel beams were employed for the tests (Fig. 3). A pendulum was constructed by suspending the beam from an overhead girder using the 300 × 50 × 10 mm steel plates welded to either ends of the beam. Four 6 mm diameter steel cables were used to construct the pendulum. Four 50 × 50 × 3 mm plates were welded to the bottom of the beams. Two to four 400 x 50 x 5 mm columns could be bolted to these plates to construct a frame. A 320 x 50 x 10 mm plate was used as the foundation plate for the columns. The columns were connected to the foundation plate by another four 50 × 50 × 3 mm plates welded to its top side. The mass of the beams could be increased by adding 200 × 150 × 3 mm steel plates on top. The constructed frame is shown in Figure 4 along with the accelerometer and strain gauges.

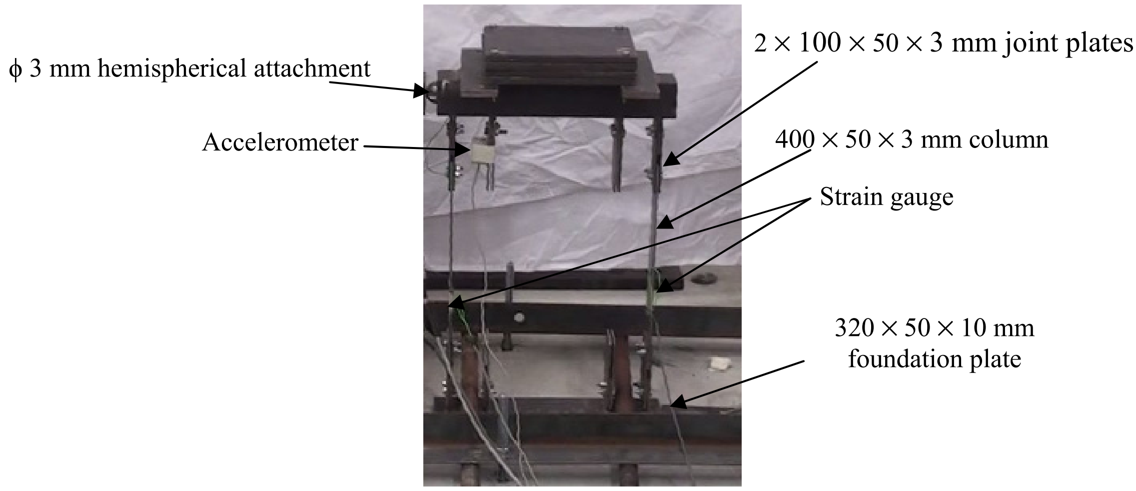

Figure 4. Frame with striker beam

A 30 mm diameter hemispherical and a plane attachment (see Fig. 4 and Fig. 3, respectively) were also fabricated. The hemispherical attachment was bolted to one beam while the plane attachment was fixed to the second beam, thus the contact occurred between a spherical and a plane surface. The tests were carried out for three different support conditions, as described in the following sub-sections.

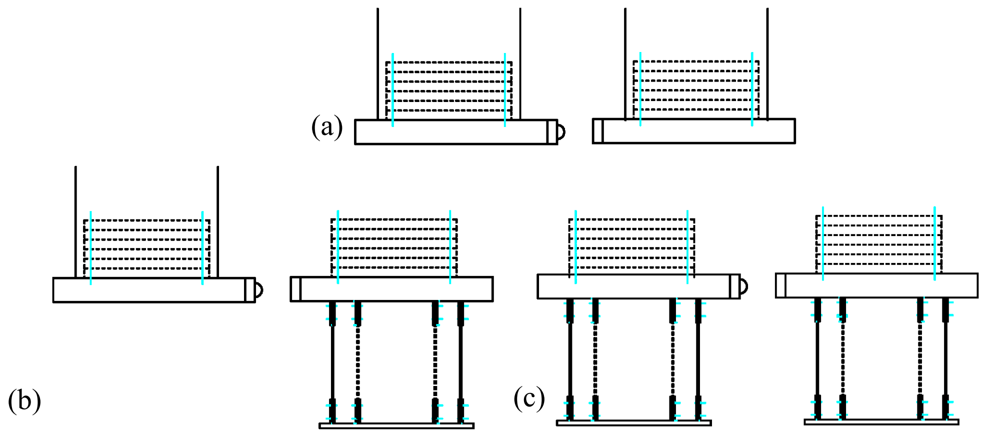

Figure 5. Test setups for impact test, with dashed-lines showing additional masses and columns. (a) impact between pendulums, (b) impact between a pendulum and a frame, and (c) impact between two frames.

2.1 Impact between pendulums

The two impacting beams were suspended from an overhead beam as pendulums such that there was less than 1 mm separation between their ends (Fig. 5a). The length of the pendulum was 2.03 m. The beam with the hemispherical attachment was displaced a certain distance and released, causing it to strike the second beam when it returned to the equilibrium position. A laser sensor was used to measure the displacement of each beam. A ± 10g Crossbow accelerometer was used to measure their acceleration. The velocity of the striker prior to impact was calculated from the initial displacement using the expressions governing the motion of a simple pendulum. The post-impact velocity of the beams was calculated from the maximum displacement after the first impact. The beams were 8.6 kg and 8.65 kg, respectively, with mass of the plane and the hemispherical elements included.

2.2 Impact between a pendulum and a frame

The struck beam in the pendulum experiments was assembled into a frame (Fig. 5b). From free vibration tests, the natural period and damping of the frame was 0.133 s and 0.5 %, respectively. The two beams were arranged end to end as in the pendulum impact, and the impact was induced by pulling and releasing the pendulum. The pendulum displacement was measured by the laser sensor while the frame displacement was measured by a strain gauge attached to the columns as shown in Figure 3. The post impact velocity of the beam supported by the columns was calculated from the maximum displacement after the first impact using the free vibration relationship for the frame.

2.3 Impact between two one-story frames

The striker beam was also attached to the columns. The natural period and damping, measured to three decimals, was same as the first frame. The two frames were placed so that their beams were very close, as in the previous two set ups. The impacts were conducted by plucking the new frame. The initial separation and initial displacement were obtained from the striker's displacement time history. The pre- and post-impact velocities of the beams were calculated from the displacement time histories of the frames. The mass of the beams with the connection plates and half of the column masses was 10.01 kg and 10.06 kg, respectively, for striker and struck beam.

The test results reported in this study are obtained from impacts between beams with no additional mass plates. The tests were repeated ten times at different initial displacements for each setup. No additional mass plates were added to the beam in the No permanent deformation was observed in the beams, the attachments or the columns during or after the test. The acceleration and displacement were recorded at 50 kHz sampling rate.

3 RESULTS AND DISCUSSION

3.1 Impact between pendulums

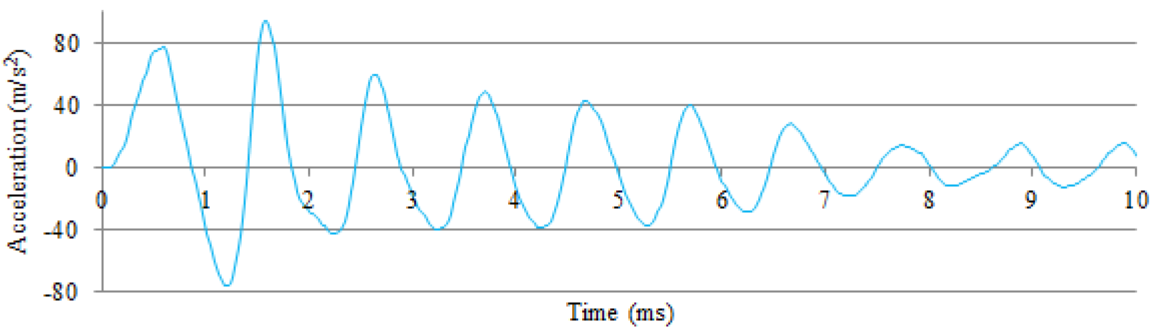

Figure 6. Acceleration of the striker for the impact between two pendulums with a relative impact velocity of 0.037 m/s

The striker's acceleration response when the initial displacement of the striker pendulum was 17 mm is shown in Figure 6. The striker became stationary after the first impact and moved only after the struck beam swung back and struck it. The struck beam attained a maximum post-impact displacement of 13 mm between the first and second contacts. The coefficient of restitution was calculated to be 0.76. This acceleration record, with multiple oscillations of large magnitudes is significantly different from past experimental results (e.g. Jankowski 2010; van Mier *et al.* 1991), which showed only one pulse. The acceleration predicted by impact force models also have only one pulse of very large magnitude acceleration after which the motion is governed by the pendulum's vibration (e.g. Khatiwada *et al.* 2014). However, similar results were obtained by the authors for the impact of RC slabs (Khatiwada *et al.* 2013) and it was postulated that the periodicity could be from the internal longitudinal vibrations of the colliding masses.

3.2 Impact between pendulum and frame

The suspended beam was displaced 21 mm and allowed to hit the second beam that was supported by two columns. The resultant acceleration of the striker is presented in Figure 7. The maximum displacement of the struck beam, between the first two impacts, was 0.7 mm. The coefficient of restitution was calculated to be 0.62.

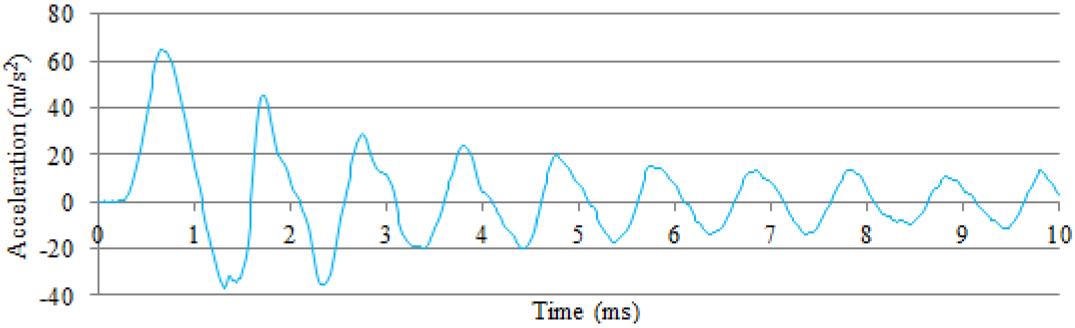

Figure 7. The acceleration of the striker pendulum's beam when the frame's beam is struck with a relative impact velocity of 0.0461 m/s

3.3 Impact between two frames

The acceleration response of the striker for the impact of two frames is shown in Figure 8. From the displacement time history of the frames, the relative impact velocity and the coefficient of restitution were calculated to be 0.107 m/s and 0.38, respectively. The oscillation period in this case was smaller than the previous ones. The acceleration time history also shows the presence of a much longer period oscillation.

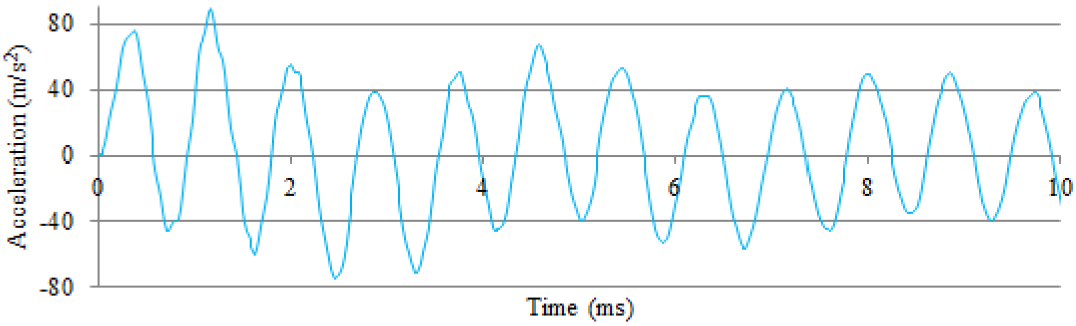

Figure 8. The striker beam's acceleration when it struck the second frame's beam at a relative impact velocity of 0.107 m/s.

Considering Figures 6–8, the support conditions had three major effects on the pounding response. As the stiffness of the pounding system increased i.e. two pendulums, a pendulum and a frame, and two frames: (i) the coefficient of restitution became smaller, (ii) the magnitude of the maximum acceleration decreased in comparison to the respective relative impact velocity, and (iii) the development of the impact acceleration changed as suggested by the shape of the time history. The ±10 g accelerometer was saturated at 0.04 m/s relative impact velocity in impact between pendulums. However, the peak acceleration is less than 8 g when the pendulum strikes a frame at 0.046 m/s velocity. In contrast, the peak acceleration was about 8.5 g when the beams of two frames collide with 0.1 m/s relative velocity.

Figure 9 presents the simulated acceleration for the cases shown in Figures 6-8, from two numerical force models; *viz.* the modified Hertzdamp model (Khatiwada *et al.* 2014) and the nonlinear viscoelastic model (Jankowski 2005). The analytical expressions for these models are provided in the relevant reference. The two models are chosen because they are both developed by adding viscoelastic damping to the nonlinear elastic Hertz contact law (Goldsmith 2001) which contains an analytically derived formula for the link stiffness for spherical to plane contact. Thus, these models should be better suited to simulate these tests while linear models have a strong disadvantage. However, Figure 9 shows that the simulations from both models are quite unlike the experimental results. The selected models could not simulate the periodicity after the first pulse or the reduction of peak acceleration magnitudes produced by the stiffer systems. Since the impact-induced acceleration is substantially overestimated for the impact between two frames, the pounding force can also be expected to be similarly overestimated. However, pounding forces have not been measured in the experiment so this cannot be verified.

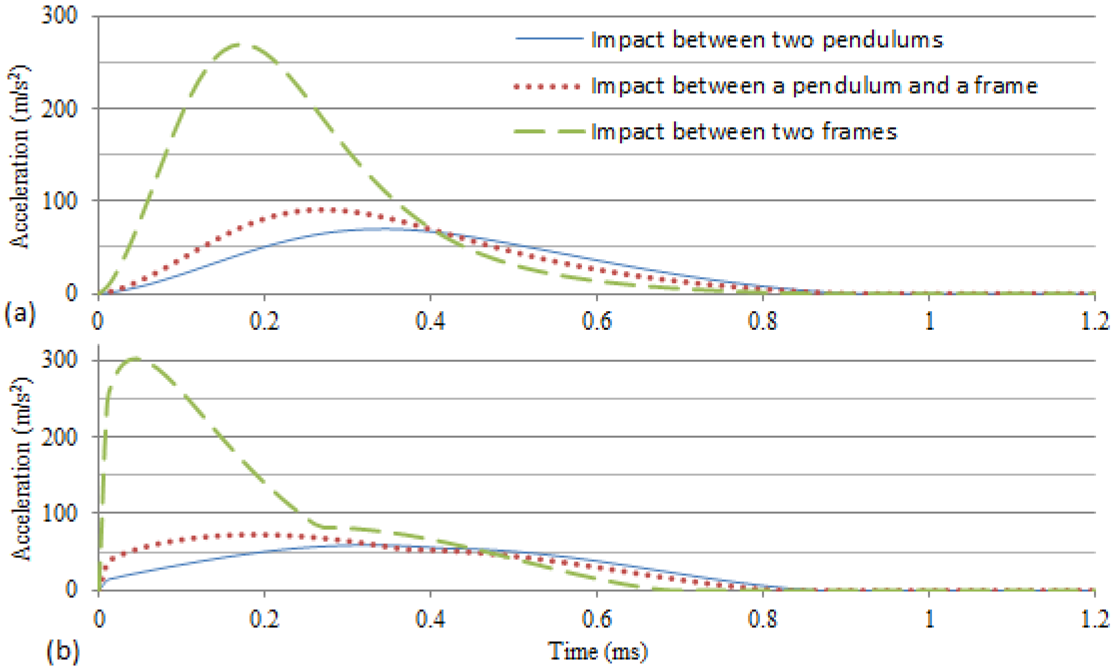

Figure 9. Numerically simulated accelerations with: (a) Hertzdamp model and (b) nonlinear viscoelastic model.

4 CONCLUSIONS

A series of experiments were conducted involving impact between two steel beams with different support conditions. Results are presented for three cases: (i) impact between two pendulums, (ii) impact between a pendulum and a steel frame, and (iii) impact between two single-storey steel frames. The numerical and experimental variations in acceleration due to the different support conditions are studied and compared. It has been shown that neglecting the contribution of the support system to the development of pounding force may results in a substantial overestimate of the structural response.

Further research will be conducted varying the masses of the beams by adding steel plates and increasing the frame stiffness by bolting additional columns to the frames.

REFERENCES

Anagnostopoulos, S.A. 1988. Pounding of buildings in series during earthquakes. *Eathquake Engineering and Structural Dynamics*, Vol **16** (3) 443-456.

Athanassiadou, C.J., Penelis, G.G. & Kappos, A.J. 1994. Seismic response of adjacent buildings with similar or different dynamic characteristics. *Earthquake spectra*, Vol **10** (2) 293-317.

Bothara, J.K., Jury, R.D., Wheeler, K. & Stevens, C. 2008. Seismic Assessment Of Buildings In Wellington: Experiences And Challenges.In *Proceedings of The 14th World Conference on Earthquake Engineering*, October 12-17, 2008. Beijing, China.

Chau, K. & Wei, X. 2001. Pounding of structures modelled as non-linear impacts of two oscillators. *Earthquake Engineering and Structural Dynamics*, Vol **30** (5) 633-651.

Chau, K.T., Wei, X.X., Guo, X. & Shen, C.Y. 2003. Experimental and theoretical simulations of seismic poundings between two adjacent structures. *Earthquake Engineering and Structural Dynamics*, Vol **32** (4) 537-554.

Chouw, N. & Schmid, G. 1995. Influence of soil-structure interaction on pounding between buildings during earthquakes. Proceeding of the 10th European Conference on Earthquake Engineering, Vienna, Austria: Balkema

Chouw, N. 2002. Influence of soil-structure interaction on pounding response of adjacent buildings due to near-source earthquakes. *JSCE Journal of Applied Mechanics*, Vol **5** 543-553.

Chouw, N. & Hao, H. 2008. Significance of SSI and nonuniform near-fault ground motions in bridge response I: Effect on response with conventional expansion joint. *Engineering Structures*, Vol **30** (1) 141-153.

Chouw, N. & Hao, H. 2012. Pounding damage to buildings and bridges in the 22 February 2011 Christchurch earthquake. *International Journal of Protective Structures*, Vol **3** (2) 123-140.

Chouw, N. & Khatiwada, S. 2013. Building pounding during earthquakes: simulations and limitations. Proceeding of Proceedings of the 10th Conference on Shock and Impact Loads on Structures, 25-26 November. Singapore.(keynote paper)

Cole, G.L., Dhakal, R.P., Carr, A. & Bull, D. 2010. An investigation of the effects of mass distribution on pounding structures. *Eathquake Engineering and Structural Dynamics*, Vol **40** (6) 641-659.

Cole, G.L., Dhakal, R.P. & Turner, F.M. 2012. Building pounding damage observed in the 2011 Christchurch earthquake. *Earthquake Engineering and Structural Dynamics*, Vol **41** (5) 893-913.

Filiatrault, A., Wagner, P. & Cherry, S. 1995. Analytical prediction of experimental building pounding. *Earthquake Engineering & Structural Dynamics*, Vol **24** (8) 1131-1154.

Goldsmith, W. 2001. In *Impact: the theory and physical behaviour of colliding solids*. New York, Dover Pubns.

Hamada, M., Nakamura, S., Ohsumi, T., Megro, K. & Wang, E. 1999. The 1999 Ji-Ji earthquake, Taiwan- investigation into damage to civil engineering structure. *Japan Society of Civil Engineering*, 160.

Hao, H. & Zhang, S.R. 1999. Spatial ground motion effect on relative displacement of adjacent building structures. *Earthquake Engineering and Structural Dynamics*, Vol **28** (4) 333-349.

Jankowski, R. 2005. Nonlinear viscoelastic modelling of earthquake induced structural pounding. *Earthquake Engineering and Structural Dynamics*, Vol **34** (6) 595-611.

Jankowski, R. 2010. Experimental study on earthquake-induced pounding between structural elements made of different building materials. *Earthquake Engineering and Structural Dynamics*, Vol **39** (3) 343-354.

Jeng, V. & Tzeng, W. 2000. Assessment of seismic pounding hazard for Taipei City. *Engineering Structures*, Vol **22** (5) 459-471.

Kasai, K. & Maison, B.F. 1997. Building pounding damage during the 1989 Loma Prieta earthquake. *Engineering Structures*, Vol **19** (3) 195-207.

Khatiwada, S., Chouw, N. & Butterworth, J.W. 2013a. Evaluation of numerical pounding models with experimental validation. *Bulletin of the New Zealand National Society for Earthquake Engineering*, Vol **46** (3) 117-130.

Khatiwada, S., Chouw, N. & Larkin, T. 2013b. An experimental study on pounding force between reinforced concrete slabs. Proceeding of Australian Earthquake Engineering Society Conference, 15-17 November. Hobart, Australia.

Khatiwada, S., Chouw, N. & Butterworth, J.W. (2014). A generic structural pounding model using numerically exact displacement proportional damping. *Engineering Structures*. **Vol 62-63** 33-41.

Li, B., Bi, K., Chouw, N., Butterworth, J.W. & Hao, H. 2012. Experimental investigation of spatially varying effect of ground motions on bridge pounding. *Earthquake Engineering and Structural Dynamics*, Vol **41** (14) 1959-1976.

Malhotra, P. 1998. Dynamics of seismic pounding at expansion joints of concrete bridges. *Journal of Engineering Mechanics*, Vol **124** (7) 794-802.

Papadrakakis, M., Mouzakis, H., Plevris, N. & Bitzarakis, S. 1991. A Lagrange multiplier solution method for pounding of buildings during earthquakes. *Earthquake Engineering and Structural Dynamics*, Vol **20** (11) 981-998.

Papadrakakis, M. & Mouzakis, H.P. 1995. Earthquake simulator testing of pounding between adjacent buildings. *Earthquake Engineering and Structural Dynamics*, Vol **24** (6) 811-834.

Rosenblueth, E. & Meli, R. 1986. The 1985 earthquake: causes and effects in Mexico City. *Concrete*

International, Vol **8** (5) 23-34.

van Mier, J., Pruijssers, A., Reinhardt, H. & Monnier, T. 1991. Load Time Response of Colliding Concrete Bodies. *Journal of Structural Engineering*, Vol **117** (2) 354-374.